Journal of Catalysis **184,** 68–76 (1999)
Article ID jcat.1999.2425, available online at http://www.idealibrary.com on IDEAL®

Synthesis, Characterization, and Activity Studies of $V_2O_5/ZrO_2–SiO_2$ Catalysts

Jack M. Miller[1] and L. Jhansi Lakshmi

Department of Chemistry, Brock University, St. Catharines, Ontario, Canada L2S 3A1

Received June 30, 1998; revised January 15, 1999; accepted January 19, 1999

A porous $ZrO_2–SiO_2$ mixed oxide catalyst support was synthesized by a sol-gel method using 2,4-pentane dione as the complexing agent. A series of supported vanadia catalysts with V_2O_5 contents ranging from 1–10 wt% were prepared using the $ZrO_2–SiO_2$ mixed oxide as the support. Characterization techniques such as BET surface area, solid-state ^{51}V and ^1H MAS NMR, and diffuse reflectance FT-IR were employed for the structural elucidation studies of the support and catalysts. Partial oxidation activities of the catalysts were determined using ethanol oxidation as the model reaction. ^{51}V NMR studies indicated the presence of tetrahedally coordinated vanadate species at lower vanadia contents and octahedral vanadyl species at higher V_2O_5 loadings. ^1H MAS NMR spectra showed peaks corresponding to hydroxyl groups of zirconia and silica. Ethanol partial oxidation activities of the catalysts indicated higher acetaldehyde selectivity for the V/Zr–Si catalysts in comparison to the V_2O_5/ZrO_2 and V_2O_5/SiO_2 catalysts.

Key Words: **sol-gel; $ZrO_2–SiO_2$; vanadia; characterization; solid-state NMR; DRIFTS; ethanol oxidation.**

INTRODUCTION

Mixed oxides synthesized by the sol-gel and coprecipitation methods have been employed as catalysts and as supports to disperse and stabilize the active phases such as metals and metal oxides. The sol-gel process offers the unique advantage of synthesis of mixed binary oxides with M–O–M' bonds. The charge imbalance of the metal ions in the M–O–M' bonds in some binary oxides was found to result in the increased acidity of the materials (1, 2). The synthesis, spectroscopic characterization of $TiO_2–SiO_2$ mixed oxide and its catalytic activity for the epoxidation reactions, was investigated by various researchers (3, 4). Zirconia–silica mixed oxides synthesized by the sol-gel method were employed for various acid catalyzed reactions such as cyclohexanol dehydrogenation (5), dehydration and dealkylation reactions (6), CO hydrogenation to isobutane and isobutene (7), and alkene isomerization (8, 9). Miller and co-workers (8, 9) have noticed that small amounts of SiO_2 in $ZrO_2–SiO_2$ aerogels prevent a loss in surface area and phase transformation of zirconia. They observed that the replacement of the TEOS precursor with the more active TMOS or the addition of acetyl acetonate to the zirconia precursor during the sol-gel synthesis to control the precursor reactivity results in higher homogeneity and catalytic activity. Moon *et al.* (10) employed $ZrO_2–SiO_2$ binary oxides with varying zirconia content synthesized by the sol-gel method for the isomerization of 2-butene. Toba *et al.* (11) synthesized $ZrO_2–SiO_2$ mixed oxides using different preparative techniques such as coprecipitation, hydrogel kneading, and complexing agent assisted sol-gel method. Zr–O–Si bond formation indicating homogeneous mixing of $ZrO_2–SiO_2$ was observed in the oxides made by the sol-gel method. The complexing/modifying agent added during the sol-gel hydrolysis would control the rate of hydrolysis of the more "active" alkoxide precursor resulting in the uniform mixing of the components. Zirconia dispersed on high surface area and thermally stable supports such as alumina or silica was subjected to investigation by various researchers (12–16). By dispersing zirconia on these commercial supports, inexpensive high surface area and thermally stable supports were produced, retaining the unique properties of zirconia–surface acid-base and redox characteristics.

The mixed metal oxides such as $TiO_2–Al_2O_3$, $TiO_2–SiO_2$, and $TiO_2–ZrO_2$ synthesized either by the sol-gel method or the conventional coprecipitation technique were employed as the supports to disperse the active vanadia phase (17–22). Handy and co-workers (17, 18) have investigated coprecipitated molecularly mixed $V_2O_5–TiO_2–SiO_2$ catalysts and vanadia supported on $TiO_2–SiO_2$ sol-gel mixed oxide for the selective catalytic reduction of NO_x. It was observed that the higher amounts of vanadia immobilized on these high surface area supports, without the formation of V_2O_5 agglomerates, result in highly active catalysts. Mastikhin and co-workers (19–21) have employed ^{51}V and ^1H NMR for the characterization of vanadia catalysts supported on mixed metal oxides such as $TiO_2–Al_2O_3$, $TiO_2–SiO_2$, and $TiO_2–ZrO_2$. Of the various spectroscopic techniques employed for the characterization of supported

[1] To whom correspondence should be addressed.

0021-9517/99 $30.00

vanadia catalysts, solid- state ^{51}V NMR provides a valuable source of structural information on the local coordination geometry of vanadia species in the catalysts. ^{51}V nucleus is very amenable for the solid-state NMR because of its high abundance (99.8%) and large nuclear magnetic moment and shorter spin lattice relaxation times. NMR experiments such as static wide-line, magic angle spinning, and quadrupolar echo techniques were employed earlier to characterize the supported vanadia catalysts. The ^1H MAS NMR technique has been used in recent years as a complementary technique with infrared spectroscopy to obtain qualitative and quantitative information of hydroxyl groups in carriers and catalysts. Diffuse reflectance FT-IR spectroscopic studies on mixed oxides and vanadia catalysts supported on these oxides were found to provide useful information regarding the presence of M–O–M' bonds and different types of hydroxyl groups in the catalysts and carriers and also to determine various kinds of vanadia species. Miller and co-workers (8, 9) and Handy and co-workers (17, 18) have employed DRIFTS to characterize the mixed oxide supports and catalysts. This technique was also employed to characterize zirconia-coated alumina and silica supports to observe the formation of Zr–O–M bonds (13–16). In the present investigation ZrO_2–SiO_2 synthesized by a sol-gel method was used as a support to disperse and stabilize the active vanadia phase. The zirconia–silica mixed oxide and vanadia catalysts were investigated employing spectroscopic techniques such as ^{51}V solid-state–static and MAS NMR, ^1H MAS NMR, DRIFT and BET surface area, and pore size distribution. The activities of the catalysts were determined using ethanol partial oxidation as the model reaction.

EXPERIMENTAL

Zirconia–silica mixed oxides were synthesized using 2,4-pentane dione as the complexing agent. The details of the preparation method are given elsewhere (23). The solvents from Caledon Laboratory and the chemicals from Aldrich were used as received. Zirconium isopropoxide (0.1 mol) and tetraethyl orthosilicate (0.1 mol) were dissolved in 200 ml of *n*-propanol followed by heating at 343 K to get a clear solution. The complexing agent, 2,4-pentane dione (0.5 mol/mol alkoxide), was added to this clear solution followed by hydrolysis with deionized water (11.0 mol/mol alkoxide). The transparent gel obtained was aged at ambient temperature for 12 h. The solvent was removed at 383 K and after drying the mixed oxide was finely powdered and then calcined at 773 K to remove the organic residues. A series of catalysts with varying vanadia content were prepared by impregnating calculated amounts of vanadium (III) acetyl acetonate (Gelest, Inc.) dissolved in methanol on the ZrO_2–SiO_2 support. The solvent was removed by rotary evaporation. The catalysts were dried at 383 K overnight followed by calcination at 773 K for 5 h. Vanadia catalysts supported on commercial ZrO_2 (Aldrich, BET surface area 30 m^2/g) and on SiO_2 (Aesar, BET surface area 215 m^2/g) were synthesized using a similar preparation procedure. The V_2O_5 contents of these catalysts and their surface areas are included in Table 1. The vanadia contents of the catalysts were estimated by inductively coupled plasma (ICP) analysis using a Perkin Elmer Optima 3300 DV ICP-OES instrument. A weighed amount of the sample was digested in hot concentrated nitric acid until the dissolution was complete and then the solution was diluted to ~2% (v/v HNO_3) prior to analysis.

TABLE 1

BET Surface Areas of the Catalysts as a Function of V_2O_5 Composition

Catalyst (wt% V_2O_5)[a]	Catalyst code	Surface area m^2/g
ZrO_2–SiO_2	Zr–Si	294
1.5% V_2O_5/ZrO_2–SiO_2	V/Zr–Si 1	288
2.5% V_2O_5/ZrO_2–SiO_2	V/Zr–Si 2	254
5.6% V_2O_5/ZrO_2–SiO_2	V/Zr–Si 3	249
6.5% V_2O_5/ZrO_2–SiO_2	V/Zr–Si 4	241
8.8% V_2O_5/ZrO_2–SiO_2	V/Zr–Si 5	229
8.0% V_2O_5/ZrO_2	V/Zr	18
9.0% V_2O_5/SiO_2	V/Si	201

[a] V_2O_5 contents of the catalysts estimated from ICP analysis.

BET surface areas of the mixed oxide and supported vanadia were determined using a Coulter SA 3100 instrument and an automated gas volumetric method employing nitrogen as the adsorbate at 77 K. The calcined samples were outgassed under vacuum at 473 K for 1 h immediately prior to analysis. Solid-state and MAS NMR experiments were carried out on a Bruker Avance DPX 300 multinuclear FT-NMR instrument. A standard bore Bruker MAS/CPMAS probe with 4-mm zirconia rotors was used. ^{51}V static and MAS spectra were obtained at 78.9 MHz with a pulse length of 1.25 μs and relaxation delay of 1 s over a spectral window of 149 kHz. The chemical shifts were referenced to $VOCl_3$ ($\delta = 0$ ppm), using V_2O_5 ($\delta = -320$ ppm) as the secondary reference. MAS spectra were recorded using variable spinning speeds ranging from 6 to 10 kHz to determine the isotropic chemical shifts. The samples were dehydrated at 623 K for 30 min in a flow of He in BET apparatus and then immediately transferred to a N_2 atmosphere glove bag and packed in zirconia rotors prior to recording the ^{51}V NMR and ^1H MAS NMR spectra. ^1H MAS NMR spectra were recorded at 300 MHz with a 30° pulse, the pulse length of 3 μs with 1 s delay between the pulses over a spectral window of 120 kHz. The chemical shifts in ppm were referenced to external TMS using neat *p*-dioxane as a secondary reference. The samples were spun at 10 kHz and 124 FIDs were accumulated for each sample. DRIFTS

spectra were acquired using a SPECTRATECH DRIFT accessory, "the collector," in an ATI Mattson Research Series FT-IR spectrometer (KBr beamsplitter, DTGS detector, spectral range 6000–400 cm^{-1}). The diffuse reflectance FT-IR spectra were recorded after evacuating the samples at 623 K and under reduced pressures in a controlled environmental chamber.

Activity studies for the partial oxidation of ethanol were carried out at atmospheric pressure in a fixed bed microcatalytic reactor interfaced to a gas chromatograph with a six-way gas sampling valve. Then, 200 mg of catalyst diluted with an equal amount of 0.5-mm glass beads were held at the middle of a 6-mm o.d. pyrex reactor between two layers of quartz wool. The catalysts were pretreated in a stream of purified dry air for 1 h at the maximum reaction temperature (573 K). After reducing the temperature to 423 K, ethanol was introduced into the reactor by flowing air (60 cc/min) through a saturator maintained at 293 K. The outlet of the reactor to the gas chromatograph was heated at 423 K to avoid condensation of the products. The catalytic runs were done in the temperature range 423–573 K; a lower reaction temperature run was repeated for all the catalysts after the highest temperature run to observe if there is any catalyst deactivation while obtaining the activity data. After a steady-state period of 30 min at each temperature the products were analyzed on-line using a Perkin Elmer Sigma 3 B gas chromatograph employing Porapaq QS (stainless steel column, 80/100 mesh, 6 ft × 0.125 in. diameter) and a thermal conductivity (TC) detector. The total concentration of CO and CO_2 was calculated as CO_x from carbon balance. Conversion was calculated as mol% ratio of ethanol reacted to ethanol fed and selectivity as mol% ratio of each product formed to ethanol reacted. The product stream comprised mainly acetaldehyde with traces of ether, acetic acid, ethyl acetate, diethoxyethane, and CO and CO_2.

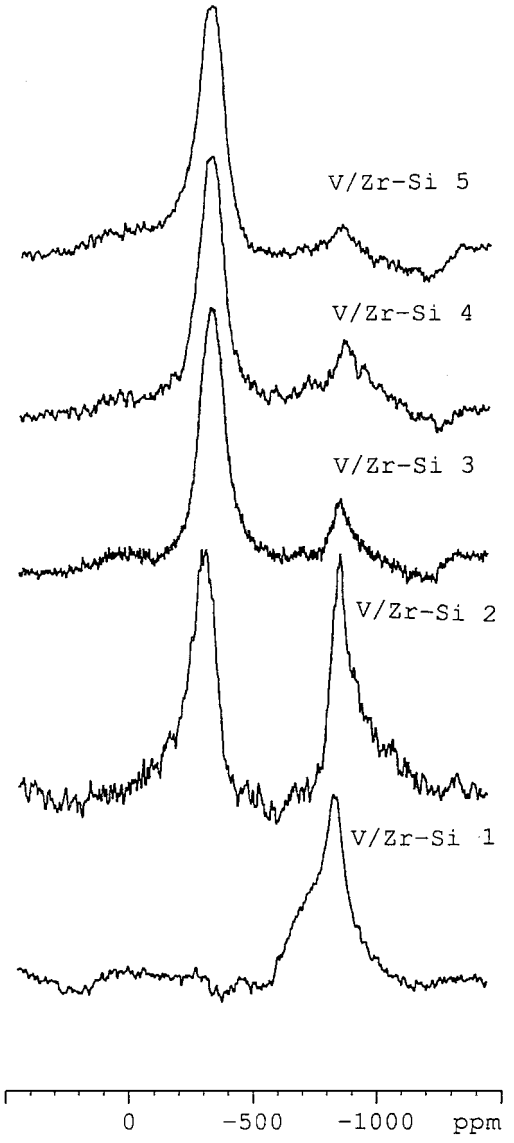

FIG. 1. 78.9 MHz solid-state ^{51}V NMR spectra of catalysts following dehydration in a flow of He at 623 K for 30 min.

RESULTS AND DISCUSSION

The BET surface area, pore volume distribution studies of the ZrO_2–SiO_2 mixed oxides were discussed earlier (23). The nitrogen adsorption isotherms of ZrO_2–SiO_2 sol-gel mixed oxide exhibited type II hysteresis loops, indicating the microporous nature. The surface areas of the catalysts are given in Table 1 as a function of catalyst composition. It can be seen that with the increase in vanadia loading there is a decrease in the surface area of the catalysts, which is expected due to the blockage of the pores of the support.

Solid-state static ^{51}V NMR spectra of the V_2O_5/ZrO_2–SiO_2 catalysts are shown in Fig. 1. The MAS spectra of the various samples are shown in Fig. 2. The isotropic chemical shifts determined with varying spin rates are given in Table 2. The peak at −785 ppm in the V/Zr–Si 1 and 2 samples, corresponds to distorted tetrahedral vanadate species and the peak at −630 ppm in the V/Zr–Si 2 catalyst can be attributed to the distorted octahedral vanadyl species. With an increase in vanadia loading, in the samples V/Zr–Si 3, 4, and 5 only the peak at −628 ppm could be seen. In the sample V/Zr–Si 1 with a V_2O_5 content of 1.5 wt%, the peak centered at −832 ppm (Fig. 1) can be assigned to distorted tetrahedral vanadate species. The tetrahedral state with a resonance at −832 ppm is not typical for vanadia catalysts supported on SiO_2 or ZrO_2 carriers (24, 25). The broadness of the peak indicates that the signal is not due to either monomeric (Q^0) or dimeric (Q^1) species since these species show only small differences between chemical shift components $\delta_\perp$ and $\delta_\parallel$. The wide chemical shift distribution indicates the presence of polymeric vanadium atoms (Q^2) in a

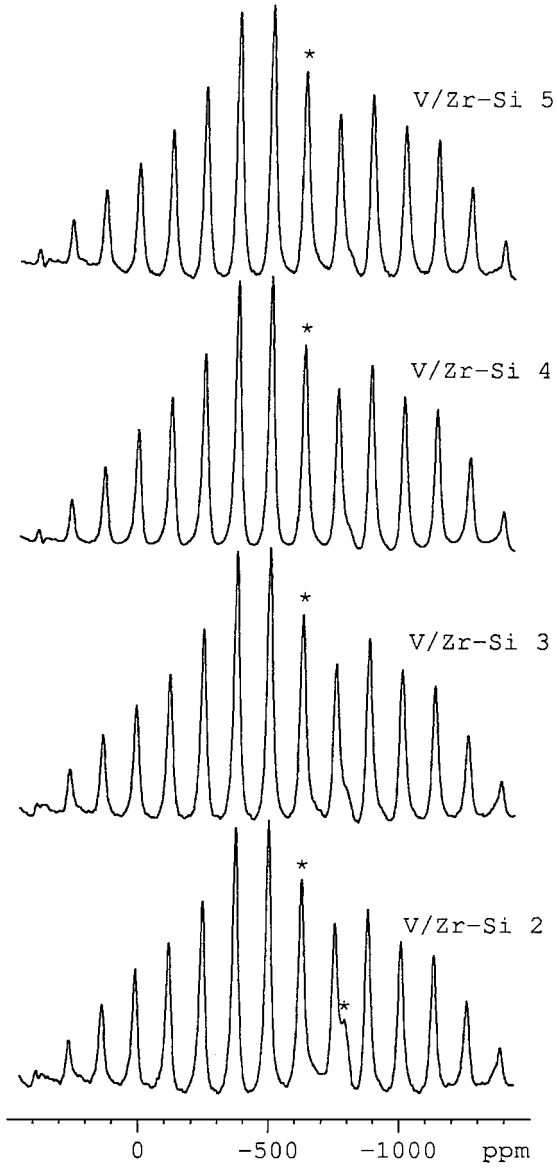

FIG. 2. ^{51}V MAS NMR spectra of dehydrated V–Zr samples (at 10 kHz spinning rate). The central resonances are indicated by the symbol ∗.

distorted tetrahedral environment. Lapina *et al.* (21) have attributed this chemical shift to ZrV_2O_7 species. In the sample V/Zr–Si 2 the peak at −832 ppm can be attributed to tetrahedral vanadia species and the peak at −327 ppm to the distorted octahedral vanadyl species. With further increase in V_2O_5 loading in the samples V/Zr–Si 3, 4, and 5, there is a decrease in the intensity of the −835 ppm peak and an increase in the intensity of the peak at −312 ppm, showing an increase of distorted octahedral species in the catalysts.

The ^1H MAS NMR spectra of the Zr–Si support and catalysts are shown in Fig. 3. The deconvoluted spectra of the support and catalysts are shown in Fig. 4. The peak at 1.6 ppm can be assigned to Si–OH groups. The peaks at 4.8

TABLE 2

^{51}V Chemical Shifts of Nonspinning and Spinning Samples (Spectra Were Shown in Figs. 2 and 3)

Catalyst	Chemical shift (ppm) (Nonspinning samples)		Isotropic chemical shift (ppm) (MAS @ 10 kHz)
	Tetrahedral	Octahedral	
V/Zr–Si 1	−832	—	−785
V/Zr–Si 2	−832	−327	−630, −789
V/Zr–Si 3	−834	−327	−628
V/Zr–Si 4	−834	−312	−628
V/Zr–Si 5	−834	−312	−628

and 2.4 ppm correspond to hydroxyl groups of ZrO_2. Similar assignments were made by Mastikhin *et al.* (26) in their ^1H MAS NMR studies on ZrO_2. In another investigation (27) they observed the peaks at 3–6 ppm; the peaks at low field were assigned to terminal –OH and the ones at high field to the bridged OH groups. Kytokivi and co-workers (13) also made similar observations in their ^1H MAS NMR studies on ZrO_2 modified silica. They noticed peaks at 1.5 and ∼5 ppm corresponding to hydroxyl groups of silica and

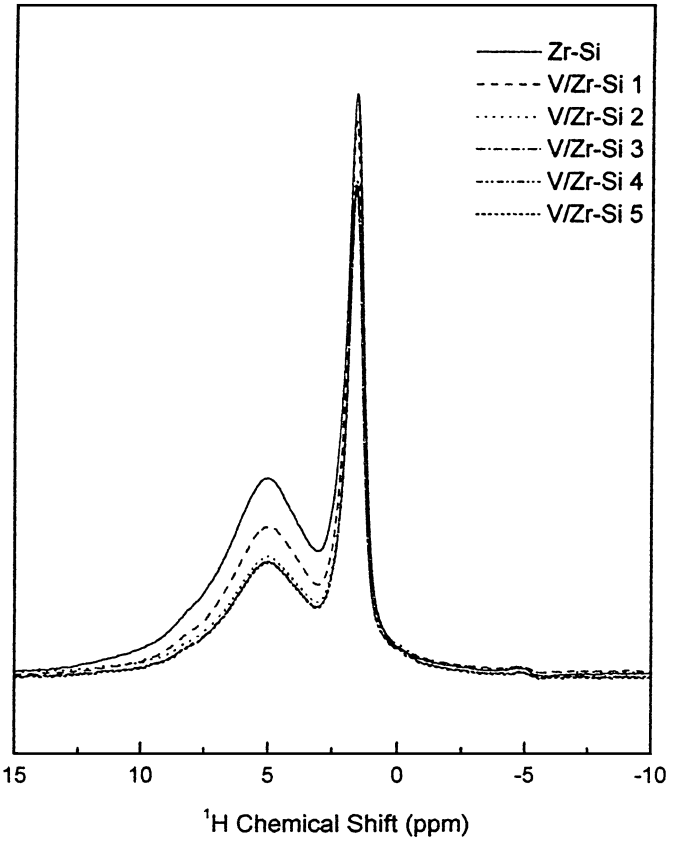

FIG. 3. ^1H MAS NMR spectra of the ZrO_2–SiO_2 support and catalysts following dehydration in a flow of He at 623 K for 30 min.

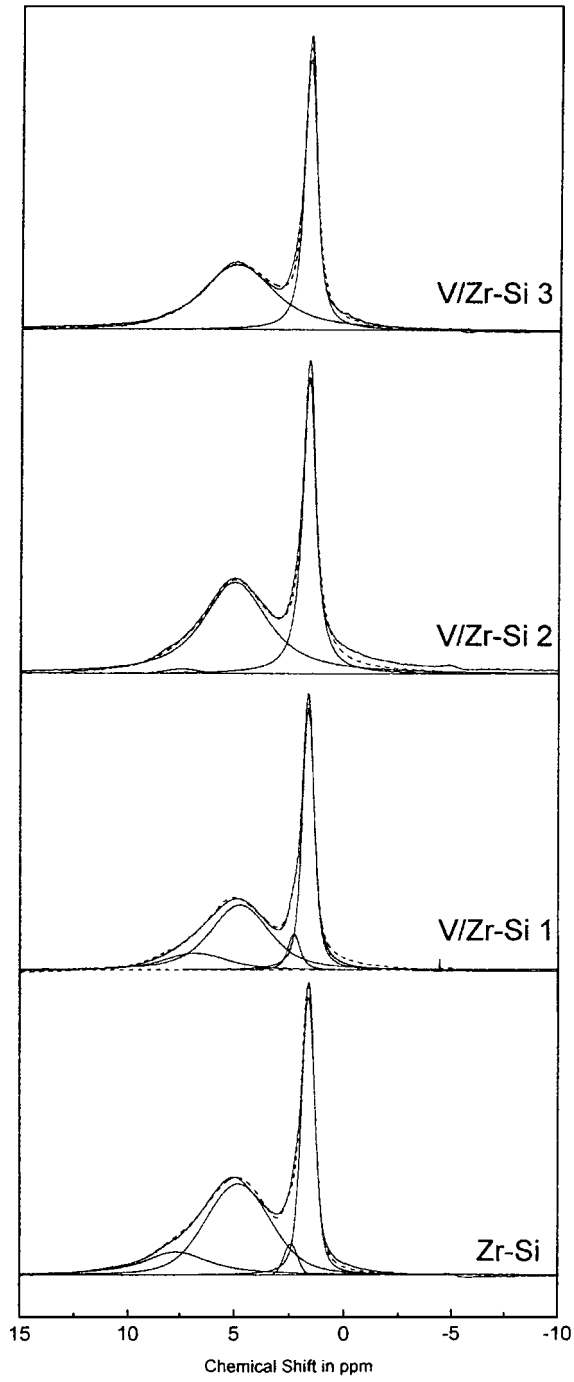

FIG. 4. Deconvoluted ^{1}H MAS NMR spectra of the Zr–Si, V/Zr–Si 1, V/Zr–Si 2, and V/Zr–Si 3. (—) Experimental spectrum; (----) curve fitted spectrum.

zirconia, respectively. Reimer *et al.* (28) observed peaks at 1.6 and 3.86 ppm in the ZrO_2 obtained from the calcination of $Zr(OH)_4$. Similar observations were made by Lapina *et al.* (20, 24) in their ^{1}H MAS NMR studies on SiO_2 and TiO_2 modified silica supported vanadia catalysts. The resonance at 1.4 ppm was assigned to Si–OH and the peaks at 2.2 and 3.2 ppm were attributed to Si–OH groups undergoing weak and strong hydrogen bonding respectively. The isolated Si–OH groups and Si–OH groups undergoing weak hydrogen bonding were found to interact with TiO_2 or V_2O_5 species. Vanadia was shown to interact with the terminal Si–OH groups as well as with the Ti–OH groups.

The diffuse reflectance FT-IR spectra of the 623 K evacuated catalysts are given in Fig. 5. Silica was known to exhibit asymmetric stretching vibrations ν_{asym} of Si–O–Si groups at 1180 and 1108 cm^{-1} and a corresponding symmetric stretching vibration ν_{sym} at 803 cm^{-1}. In the 473 K outgassed Zr–Si sample, major vibrations were observed at 943 and 1197 cm^{-1}. Upon increasing the outgassing temperature to 623 K, the broadness of the bands decreased and vibrations were observed at 985, 1055, and 1187 cm^{-1}. The vibration at 985 cm^{-1} corresponds to Si–OH groups. There may be an overlap of bands at 950 cm^{-1} corresponding to Zr–O–Si bonds (8, 13, 14). Similar assignments were made for Ti–Si samples where the IR vibration at 945 cm^{-1} was assigned to Si–O–Ti linkage (29). The IR vibrations of 623 K outgassed samples are given in Table 3. In the samples V/Zr–Si 1 and V/Zr–Si 2 a peak at ~926 cm^{-1} indicates highly dispersed vanadate species, isolated VO_4^{3-} tetrahedra (30). At higher vanadia contents in the samples V/Zr–Si 4 and V/Zr–Si 5, several sharp vibrations were noticed, probably corresponding to vanadia species in lower coordination environments. The deconvoluted spectra of the V/Zr–Si 4 and 5 are given in Fig. 6. The vibrational bands were observed at 928, 950, 978, and 1019 cm^{-1} corresponding to the decavanadate species (31). There may be overlap of vibrations from Zr–O–Si and Si–OH bonds with the bands at 950 and 980 cm^{-1}, respectively. The vibration at 737 cm^{-1} can be attributed to the V–O–V stretching band (32). The band at 1020 cm^{-1} corresponds to $\nu_{V=O}$. The DRIFTS studies of the catalysts are in support with the ^{51}V NMR results, where tetrahedral vanadate species were noticed at lower loadings and at higher V_2O_5 contents the peaks corresponding to both tetrahedral vanadate and distorted octahedral vanadyl species were noticed.

Figure 7 shows the DRIFT spectra of the catalysts 623 K evacuated catalysts in the hydroxyl region. In the

TABLE 3

The DRIFTS Vibrations for the Zr–Si and the V/Zr–Si Catalysts Shown in Fig. 5

Sample	Wave number cm^{-1}					
Zr–Si	—	—	—	958	985	—
V/Zr–Si 1	—	—	925	—	—	—
V/Zr–Si 2	—	—	927	—	—	—
V/Zr–Si 3	—	857	—	951	984	1018
V/Zr–Si 4	737	842	925	953	979	1018
V/Zr–Si 5	738	846	928	954	977	1020

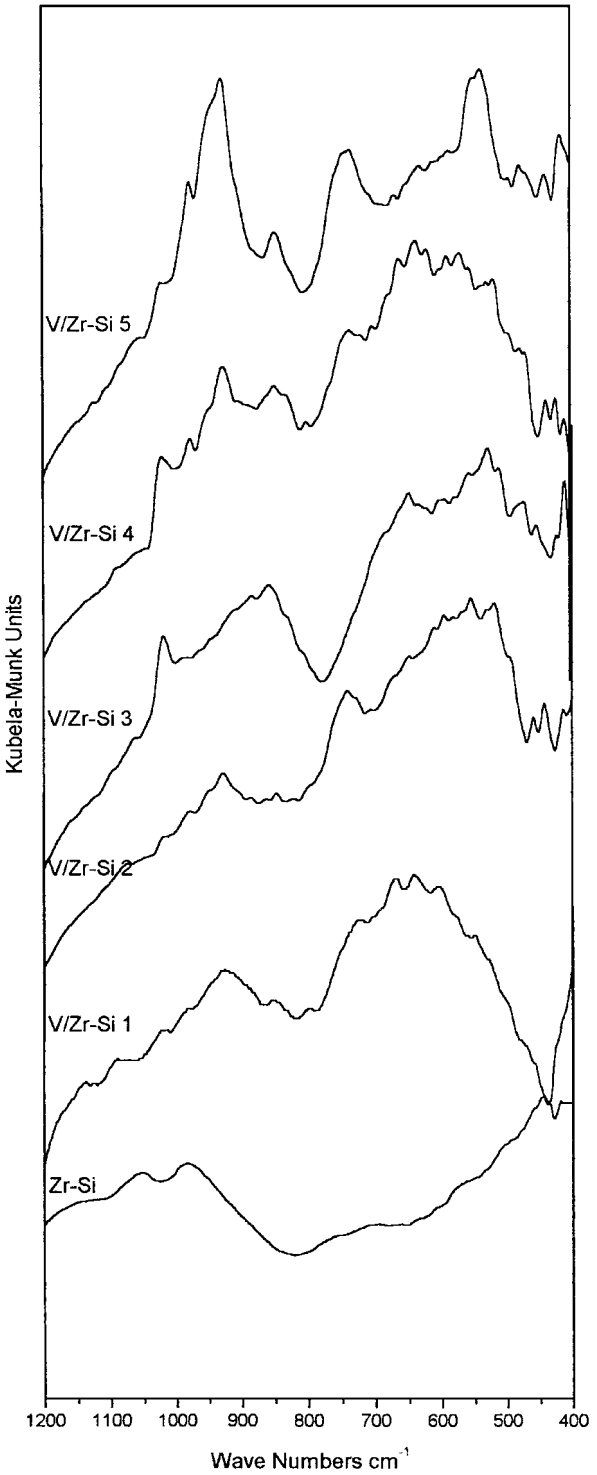

FIG. 5. Diffuse reflectance FT-IR spectra of the ZrO_2–SiO_2 support and the catalysts outgassed at 623 K for 30 min (in the 400–1200 cm^{-1} region).

calcined samples vibrations were observed at 3200, 3562, and 3730 cm^{-1}. Upon outgassing the samples at 473 K and 3546 and 3730 cm^{-1} bands were then seen. The vibration at 3730 cm^{-1} can be assigned to Si–OH based on the earlier reports (8, 14, 16, 18). The vibration at 3562 cm^{-1} can be assigned to Zr–OH vibrations. On further increasing the outgassing temperature to 623 K, the vibrations could be seen at 3721, 3604, and 3164 cm^{-1}. The peak at 3721 cm^{-1} decreased in intensity in comparison to the 473 K outgassed sample indicating the removal of some of the terminal OH groups of Si. The latter two peaks at 3604 and 3164 cm^{-1} could be assigned to zirconia hydroxyl groups. The bands at 3680 and 3670 cm^{-1} were assigned earlier (13, 14) to the vibrations of Zr–OH groups in tetragonal or monoclinic phases of ZrO_2.

Ethanol partial oxidation was employed earlier as a model reaction on supported vanadia and molybdena

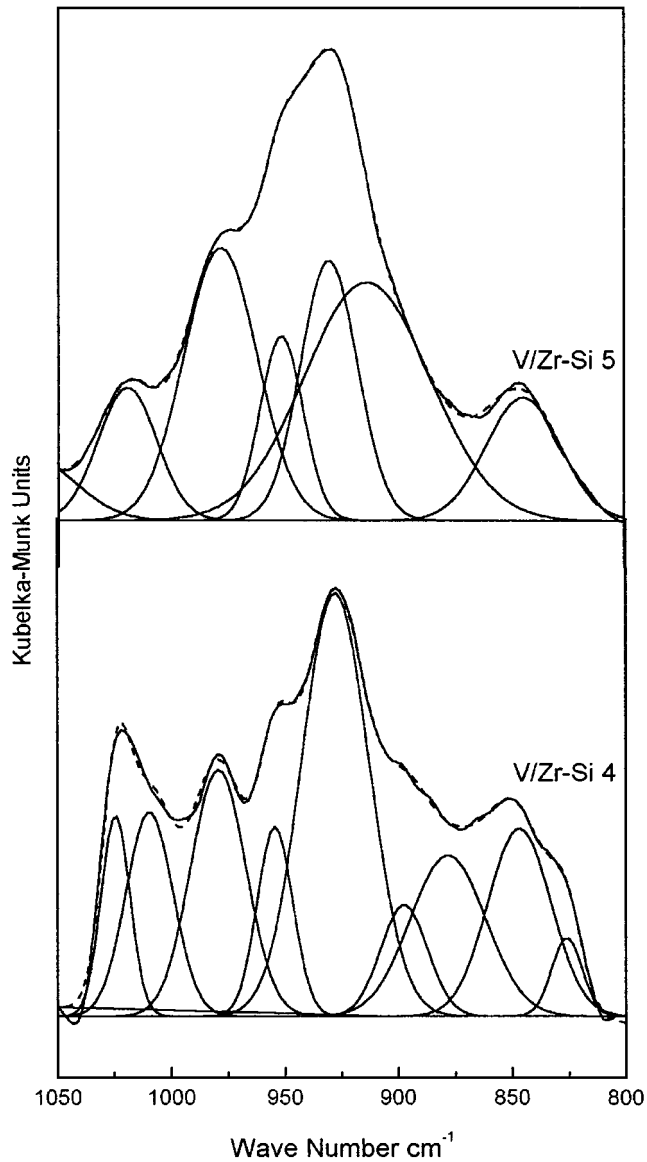

FIG. 6. Deconvoluted DRIFTS spectra of the V/Zr–Si 4 and V/Zr–Si 5 samples outgassed at 623 K for 30 min. (—) Experimental spectrum; (----) curve fitted spectrum.

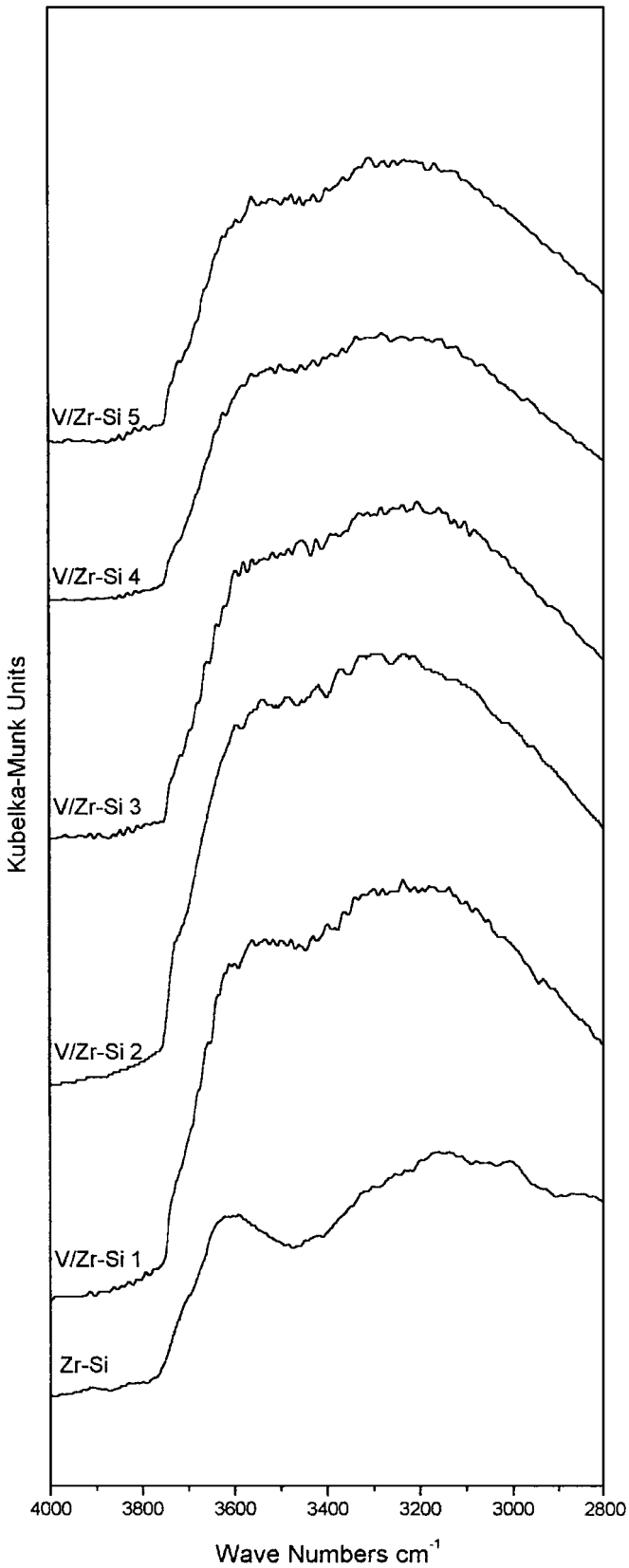

FIG. 7. Diffuse reflectance FT-IR spectra of the ZrO_2–SiO_2 support and catalysts outgassed at 623 K for 30 min. (in the hydroxyl region 2800–4000 cm^{-1}).

catalysts (33–35). Oyama and Somorjai (33) in their ethanol oxidation studies on silica supported vanadia catalysts have shown that ethanol oxidation is a structure insensitive reaction. They observed total selectivity to acetaldehyde at low reaction temperatures, to acetic acid at intermediate temperatures, and to CO_x and ethylene at high reaction temperatures. Quaranta *et al.* (34) in their ethanol oxidation studies on $V_2O_5/TiO_2/SiO_2$ catalysts observed higher acetaldehyde selectivity in comparison to V_2O_5/SiO_2 and V/TiO_2 catalysts. They attributed the increased activity and selectivity to the increased interaction of vanadia with a titania component of the modified silica support.

The ethanol partial oxidation rates of various catalysts are shown in Fig. 8 as a function of reaction temperature. It can be seen from the figure that there is no significant difference in the reaction rates of the V/Zr–Si catalysts. The V/Zr and V/Si catalysts were found to be more active than the V/Zr–Si catalysts. Commercial V_2O_5 was also tested under similar reaction conditions after calcining at 773 K for 5 h. V_2O_5 exhibited higher activity in comparison to the supported catalysts. ZrO_2 and SiO_2 supports exhibited very low conversions with total selectivity to acetaldehyde while Zr–Si exhibited total selectivity to ether, indicating the acidic nature of the Zr–Si mixed oxide support (1, 2). V/Zr–Si 1 catalyst exhibited a lower reaction rate in comparison to other catalysts, which may be due to the low V_2O_5 content. V/Zr–Si catalysts exhibited total selectivity to acetaldehyde at lower reaction temperatures; traces of ether were observed in the case of V/Zr–Si 1 and V/Zr–Si 2 catalysts. At higher reaction temperatures traces of acetic acid, ethyl acetate, ethylene, and CO_x were observed with

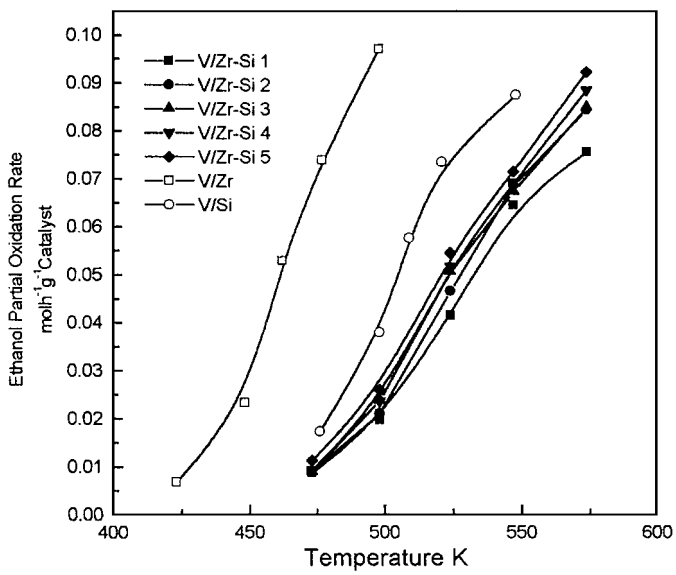

FIG. 8. Ethanol partial oxidation rates of various catalysts as a function of reaction temperature; reaction conditions were given in Experimental section.

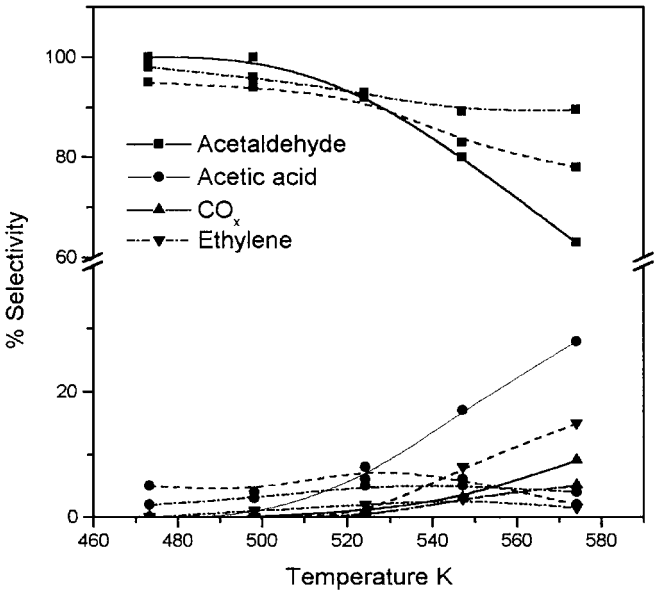

FIG. 9. Mol% selectivity to various products as function of reaction temperature for the catalyst V/Zr (—), V/Si (----), and V/Zr–Si (–·–·).

acetaldehyde as the major product. The selectivity to various products observed in the reaction for the V/Zr, V/Si, and V/Zr–Si catalysts were shown in Fig. 9 as a function of reaction temperature. As can be seen from the figure, vanadia supported on zirconia exhibited about ~28% selectivity to acetic acid at the total conversion level; at lower reaction temperatures acetaldehyde was the major product. In the case of the silica supported vanadia catalyst the selectivity to ethylene was significant at 100% conversion (~15 mol%). The V/Zr–Si vanadia catalysts exhibited acetic acid, ethylene, and CO_x as the major reaction by-products and about 90% selectivity to acetaldehyde. The acetaldehyde selectivity of the catalysts are in the order V/Zr–Si > V/Si > V/Zr at higher reaction temperatures. Thus, the present study shows that ZrO_2–SiO_2 supported vanadia catalysts are efficient for the selective dehydrogenation of ethanol to acetaldehyde.

CONCLUSIONS

^{51}V NMR studies of the catalysts indicated highly dispersed tetrahderally coordinated vanadate species at lower vanadia loading and distorted octahedral vanadyl species at higher vanadia contents. DRIFTS studies of the catalysts are in agreement with ^{51}V NMR studies; the vibrations corresponding to tetrahedral vanadate species were observed at lower loadings, while at higher V_2O_5 contents, a set of several sharp vibrations corresponding to decavanadate species was observed. The ^{1}H MAS NMR signal of zirconia–silica support indicated four types of hydroxyl groups corresponding to the terminal and bridged hydroxyl groups of zirconia and silica. Vanadia catalysts supported on a ZrO_2–SiO_2 sol-gel support were found to exhibit higher selectivity to acetaldehyde in comparison to the ZrO_2 and SiO_2 supported vanadia catalysts.

ACKNOWLEDGMENTS

Thanks are due to Prof. I. Brindle for ICP analysis and Tim Jones for his assistance during the NMR investigations. The authors thank NSERC, Canada for financial support. We also thank Dr. Chris Ratcliffe, NRC, Canada for obtaining ^{51}V NMR spectra.

REFERENCES

1. Tanabe, K., Sumiyoshi, T., Shibata, K., Kiyoura, T., and Kitagawa, K., *Bull. Chem. Soc. Jpn.* **47**, 1064 (1974).
2. Kung, H. H., *J. Solid State Chem.* **52**, 191 (1984).
3. Hutter, R., Mallat, T., and Baiker, A., *J. Catal.* **157**, 665 (1995).
4. Imamura, S., Nakai, T., Kanai, H., and Ito, T., *Catal. Lett.* **28**, 277 (1994).
5. Bosman, H. J., Kruissink, E. C., Van der Spoel, J., and Van den Brink, F. J., *J. Catal.* **148**, 660 (1994).
6. Sohn, J. R., and Jang, H. J., *J. Mol. Catal.* **64**, 349 (1991).
7. Feng, Z., Postula, W. S., Erkey, C., Philip, C. V., Akgerman, A., and Anthony, R. G., *J. Catal.* **148**, 84 (1994).
8. Miller, J. B., and Ko, E. I., *in* "Advanced Catalysts and Nanostructured Materials" (W. R. Moser, Ed.), p. 21. Academic Press, San Diego, 1996.
9. Contescu, C., Popa, V. T., Miller, J. B., Ko, E. I., and Schwarz, J. A., *J. Catal.* **157**, 244 (1995).
10. Moon, S.-C., Fujino, M., Yamashita, H., and Anpo, M., *J. Phys. Chem.* **101**, 369 (1997).
11. Toba, M., Mizukami, F., Niwa, S.-i., Sano, T., Maeda, K., Annila, A., and Komppa, V., *J. Mol. Catal.* **94**, 85 (1994).
12. Gomez, R., Lopez, T., Tzompantzi, F., Garciafigueroa, E., Acosta, D. W., and Novaro, O., *Langmuir* **13**, 970 (1997).
13. Kytokivi, A., Lakomaa, E.-L., Root, A., Osterholm, H., Jacobs, J.-P., and Brongersma, H. H., *Langmuir* **13**, 2717 (1997).
14. Dang, Z., Anderson, B. G., Amenomiya, Y., and Morrow, B. A., *J. Phys. Chem.* **99**, 14437 (1995).
15. Lopez, T., Navarrete, J., Gomez, R., Novaro, O., Figueras, F., and Armendariz, H., *Appl. Catal.* **125**, 217 (1995).
16. Damyanova, S., Grange, P., and Delmon, B., *J. Catal.* **168**, 421 (1997).
17. Handy, B. E., Maciejewski, M., and Baiker, A., *J. Catal.* **134**, 75 (1992).
18. Handy, B. E., Baiker, A., Schraml-Marth, M., and Wokaun, A., *J. Catal.* **133**, 1 (1992).
19. Mastikhin, V. M., Terskikh, V. V., Lapina, O. B., Filimonova, S. V., Seidl, M., and Knozinger, H., *J. Catal.* **156**, 1 (1995).
20. Mastikhin, V. M., Terskikh, V. V., Lapina, O. B., Filimonova, S. V., Seidl, M., and Knozinger, H., *Solid State Nucl. Magn. Reson.* **4**, 369 (1995).
21. Lapina, O. B., Mastikhin, V. M., Shubin, A. A., Krasilnikov, V. N., and Zamaraev, K. I., *Prog. NMR Spectr.* **24**, 457 (1992).
22. Rodenas, E., Yamaguchi, T., Hattori, H., and Tanabe, K., *J. Catal.* **69**, 434 (1981).
23. Miller, J. M., and Lakshmi, J. L., *J. Phys. Chem. B* **102**, 6465 (1998).
24. Lapina, O. B., Nosov, A. V., Mastikhin, V. M., Dubkov, K. A., and Mokrinski, V. V., *J. Mol. Catal.* **87**, 57 (1994).
25. Das, N., Eckert, H., Hu, H., Wachs, I. E., Walzer, J. F., and Feher, F. J., *J. Phys. Chem.* **97**, 8240 (1993).
26. Mastikhin, V. M., and Zamaraev, K. I., *Appl. Magn. Reson.* **1**, 295 (1990).

27. Mastikhin, V. M., Nosov, A. V., Filimonova, S. V., Terskikh, V. V., Kotsarenko, N. S., Shmachkova, V. P., and Kim, V. I., *J. Mol. Catal.* **101**, 81 (1995).
28. Riemer, T., Spielbauer, D., Hunger, M., Mekhemer, G. A. H., and Knozinger, H., *J. Chem. Soc. Chem. Commun.* **10**, 1181 (1994).
29. Dutoit, D. C. M., Schneider, M., and Baiker, A., *J. Catal.* **153**, 165 (1995).
30. Sanati, M., and Andersson, A., *J. Mol. Catal.* **59**, 233 (1990).
31. Day, V. W., Klemperer, W. G., and Maltbie, D. J., *J. Am. Chem. Soc.* **109**, 2991 (1987).
32. Wallenberg, L. R., Sanati, M., and Andersson, A., *J. Catal.* **126**, 246 (1990).
33. Oyama, S. T., and Somorjai, G. A., *Catal. Sci. Tech.* **1**, 219 (1991).
34. Quranta, N. E., Soria, J., Cortes Corberan, V., and Fierro, J. L. G., *J. Catal.* **171**, 1 (1997).
35. Oyama, S. T., and Zhang, W., *J. Am. Chem. Soc.* **118**, 7173 (1996).